PULSE PocketQube: Cosmic radiation analysis of the LEO environment during a solar event

Faith TNG
Technische Universität Berlin
Straße des 17. Juni 135, 10623 Berlin

Vasantha Kanesh Muruganantham
Technische Universität Berlin
Straße des 17. Juni 135, 10623 Berlin

Palaniappan Subramanian
Technische Universität Berlin
Straße des 17. Juni 135, 10623 Berlin
palaniappan.subramanian@campus.tu-berlin.de

Faculty Advisor: Cem Avsar
Technische Universität Berlin
cem.avsar@tu-berlin.de

ABSTRACT

Space weather events can cause harmful effects to spacecraft and communications in Low Earth Orbit, where the cosmic radiation environment during such an event is understudied. Real-time data that characterizes this environment in detail with respect to spatial and temporal characteristics could help us better understand particle composition and interactions in LEO during a solar event, as well as enhance existing predictive models for space mission planning. Current approaches have limited information on particle composition with respect to dose and energy rates, and are hindered by high costs in deploying large space weather monitoring constellations. This proposed satellite mission, PULSE, aims to overcome these challenges by demonstrating a 3P PocketQube equipped with a novel Timepix2 semiconductor detector that can conduct advanced radiation analysis by mapping particle flux corresponding to time of arrival and deposited energy rates for each particle, ultimately reconstructing the radiation environment during a solar event. PULSE is conceptually designed based on a unique operational concept in managing power and data link capacity within the PocketQube configuration to trigger an action that acts as a preliminary solar event alarm. Simulations of various subsystems are performed. The PULSE mission is planned for 7 months during the solar maximum event of 2025. To map the impact of particles on a LEO satellite. Eclipse time is estimated to be 35.42% of mission lifetime and additionally 6 partner ground stations are selected with average contact time of 330 seconds for telecommunications.

1. INTRODUCTION

Space weather effects, particularly near Earth, result in cosmic radiation fluctuations that can affect spacecraft electronics and satellite radio communications in Low Earth Orbit (LEO), as well as pose threats to astronaut health[1]. A notable example was the February 2022 event where Starlink lost 39 out of its 44 satellites as coronal mass ejection effects increased atmospheric drag at its staging altitude, forcing it to deorbit early. An early warning system in LEO could have pre-empted them to change course [2].

Despite this, most studies today focus on cosmic radiation threats in deep space. The cosmic radiation environment during a solar event in LEO, which has 9,900 operational satellites as of 4 May 2024, is relatively understudied. Reitz[3] identifies two primary sources of cosmic radiation in LEO.The first source is Galactic Cosmic Radiation (GCR) which originates from beyond our solar system and which primarily comprises alpha particles, and heavier ions, with intensities fluctuating according to solar activity. The second source is Solar Cosmic Radiation (SCR), which comprises high-energy particles, primarily protons and electrons that are emitted by the Sun during solar flares. During solar maximum, these solar events are more likely to happen, triggering complex interactions and introducing variability in radiation levels that complicate prediction models.

Additionally, present models that have wide coverage for monitoring these effects in LEO are based on non-real-time data such as the AE8/AP8 from the year 1980, and its successor AE9/AP9 from the year 2012, which are limited in accurately representing the radiation environment[4]. AE9/AP9 for example describes particle fluxes over spatial ranges of $0.98 < L^* < 12.4$ and $0.98 < L^* < 12.4$ respectively; covering energy ranges of 40 keV—10 MeV (electrons) and 100 keV—2 GeV (V1.20)[5]. It does not distinguish between energy and dose rates with respect to particle compositions and time of arrival. New real-time datasets are solicited to augment such models and could inform better space mission planning strategies [6]. Another barrier to real-time space weather monitoring systems is that such systems require multi-point coverage within LEO. Sending a constellation will incur high cost. Exploring a solution that uses PocketQubes could be cost-effective in the long run in deploying large constellations, because of the ability to update or replace them in comparison to larger satellites, allowing for the spatial and temporal coverage necessary for space weather monitoring [7][8]. Recent approaches to the authors' knowledge are a minimum of 1U in size and have limited information on dose rate, energy deposits, and characterisation of the radiation environment. This includes missions to measure count rate in the South Atlantic Anomaly and reconstructing radiation maps to identify solar particle events corresponding to individual particles, but not with relation to direction and time of arrival [9][10][11][12].

2. MAIN MISSION

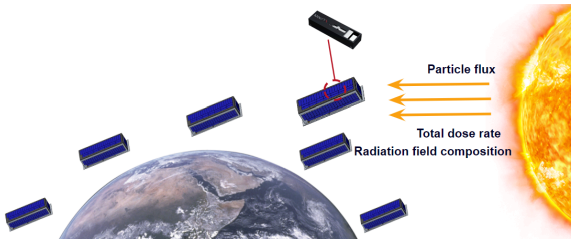

Figure 2.1. Mission concept

This mission and primary scientific objective is aimed at demonstrating PULSE, a 3P PocketQube platform to map particle flux, total dose rate and radiation field composition in LEO during a solar event, contributing direct measurements to real-time computer models and serving as a mini solar event alarm system.

PULSE will be equipped with a novel radiation semiconductor detector, the MiniPix Sprinter, which consists of a radiation camera and ASIC chip that simultaneously measures the time of arrival and deposited energy for each detected particle (alpha particles, protons, electrons and muons), providing a significant capability in providing a two-dimensional dataset gives detailed radiation analysis into particle characteristics and interactions during a solar event.

Each of its 256 x 256 pixels sensors has an amplifier and a discriminator for precise detection. It is

controlled via a USB 2.0 interface with a standard micro-USB connector to integrate seamlessly with our communication system, and comes with the PIXET PRO software compatible with our operating system, allowing us to run statistical analysis of collected data frames to collecting long exposures or data from a portion of the sensor.

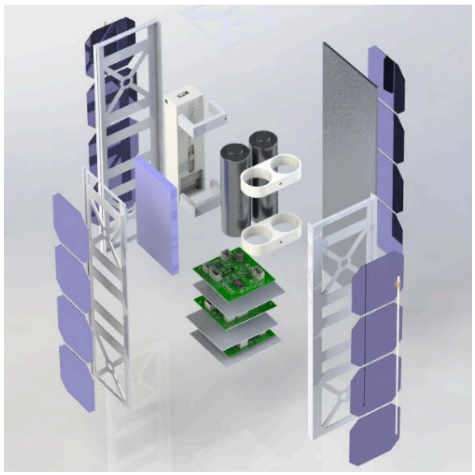

Figure 2.2. PULSE Bombarded View

The spacecraft employs a minimal architecture and sophisticated duty cycling scheme which allows for a power-intensive payload. The satellite has the capability of measuring attitude and propagation using a 9-axis IMU but does not control the attitude or orbit. PULSE will communicate with a ground station using an UHF transceiver and a deployable omnidirectional antenna. The satellite has a Linux based on-board computer for handling the platform and payload data.
The secondary objective of this project is educational in nature and aims to develop skills in spacecraft design for Masters in Space Engineering students at the Technical University of Berlin. As such a sensor has never been integrated on such a small satellite platform before, it provides a challenge as an educational project for university students to work within mass, power and volume constraints.

2.1. CONCEPT OF OPERATIONS

2.1.1. Launch & Deployment

Several factors including mission duration, particle flux and incidence count and relevance to applications were considered for deciding the ideal orbit height and parameters. To comply with the debris mitigation guidelines an altitude between 250 km to 550 km were considered. Since these are also the regions with the highest number of satellites apart from GSO [13], a higher preference is given to account for mission impact and relevance.

The exact orbit height is however determined by three major factors; particle flux, traceability and orbit decay. The AP8 model calculation of integral proton flux as a function of atmospheric density was plotted by Gautam D. Badhwar [14]. The study reveals the high energy (> 30 MeV) particle flux increases 50 times from 250 km to 500 km. At the same time the orbit decay period increases and traceability of a PocketQube reduces with increase in altitude. Considering this an orbit of 350 Km is chosen as an intermediate value.

It would be ideal to launch the satellite at the end of 2024 or early 2025 to make use of the solar maximum cycle to capture the impact of high solar activity on satellites in LEO. But, this is subjected to availability of launch and completion of satellite build and other programmatic factors.

Sun-synchronous polar orbit is selected for the following reasons:

- Smaller satellites are more prone to perturbations from atmospheric drag, sun-synchronous orbits have constant atmospheric density avoiding the mentioned perturbations
- Sun-synchronous orbits have a consistent particle flux expectation as per the beta angle, any change from the predicted value would be easier to identify
- The orbit guarantees optimal illumination for the solar panels, adequate thermal conditions and great duty cycle opportunities for communication

For ground stations, TU-Berlin's existing partner ground stations are considered to simplify operational constraints and maximize contact options:

1. Berlin (Germany)

2. Brandenburg (Germany)
3. Backnang (Germany)
4. Svalbard (Norway)
5. Buenos Aires (Argentina)
6. San Martín Base (Antarctica)

Figure 2.3. Ground Stations for Communications

Post deployment commissioning would begin post a 45 minute delay to ensure RF inhibit rules are met as per the standard protocols of deployment. PULSE uses an array of embedded air coils for attitude control. Post 45 minute delay, PULSE would perform attitude stabilization and power generation for operations.

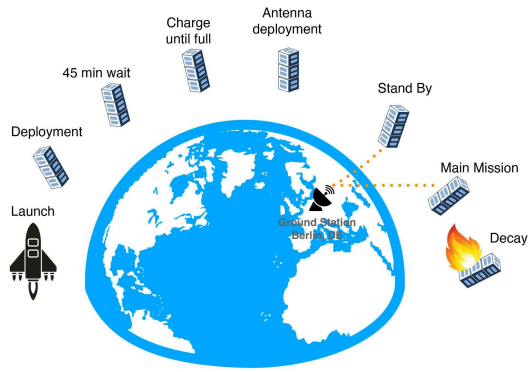

Figure 2.4. Satellite life cycle

2.1.2. Initial Checks & Traceability

PULSE is set up to perform several safety checks prior to the start of normal operations. These checks will begin after the batteries are fully charged on the first cycle.This checkout phase would include monitoring the health and attitude of the satellite to meet the operational demands of the mission. PocketQubes are extremely small and are bound to be launched in a rideshare system with multiple other similar sized objects. ‘CubeSat confusion’ is the name given to the trackability problems associated with CubeSats, this is a bigger problem in PocketQubes and hence tracking aids are incorporated in design and a community based tracking approach is incorporated.

1. PULSE position via radio - a blackbox internal mounting radio is considered for communicating positional data directly to ground
2. PULSE is also equipped with external RFID tags for easier identification and tagging

Corner reflectors and exterior mounted LEDs are not considered to maximize the area for power generation.

2.3 Operational Modes

To manage power and downlink capabilities within a PocketQube configuration, operational modes were developed for various scenarios to prioritize power allocation for significant events.

2.3.1 Science Mode

There are two different modes under science mode which utilizes the payload to detect energy particles, these are low power and full power modes depending on the selected payload strategy.

2.3.2. ADCS Mode

The science task doesn’t require attitude stabilization and is hence performed while free tumbling. The ADCS mode is incorporated to reduce the tumbling rate to below 5 degree per second for establishing stable link.

2.3.3. Link Mode

PULSE can be expected to make in between 5 to 13 passes over the GS depending on the location of GS. These are primarily used for transfer of metadata or uplink of commands. Due to power constraints, image acquisition cannot run parallel to downlink mode.

2.3.4. Standby Mode

Default mode of the satellite, where the subsystems are on and are accepting telecommands and waiting for the next task.

2.3.5 Safe Mode

A power threshold is set falling below which results in tasks termination, payload shut down and OBC and TT&C goes to sleep mode. PULSE goes on charging and consumes as little power as possible.

2.4 Image Acquisition Strategies

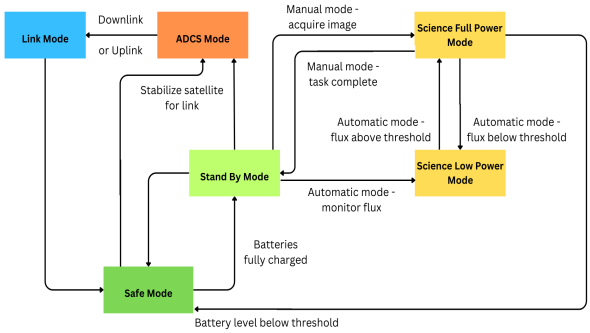

Figure 2.5. Operational Mode Transfer

2.4.1. Automatic Payload Operation

This is the default operational cycle for payload image acquisition. This consumes lower power and produces individual 'snapshots' at 1 frame per minute. The exposure time for these images is hence 1 minute, this means it is ideal for low radiation events. Hence, an independent sensor measures the solar flux rates and decides the mode of image acquisition. At this low power mode, only image metadata including information about particle count and energy is stored and sent via downlink. Once the sensor detects the flux rates above the set threshold, the payload goes into full power mode indicating significant activity, in which case images and metadata are both sent via downlink.

2.4.2. Manual Payload Operation

This will be only used in one of two scenarios, either failure of automatic payload operation or in anticipation of an event of particular interest, for example high solar activity or GCR. In this case manual start and stop times are set for image collection and transfer.

2.5. End of Life

The mission orbits and associated elements are chosen to facilitate natural decay within the stipulated period of 5 years as per the new sustainable space guidelines of ESA.
GMAT simulation of PULSE satellite with 750 grams and designated surface area and drag coefficient launched to 350 km on Epoch 1 Jan 2025 (UTC Gregorian) revealed a mission life time of 7 months.

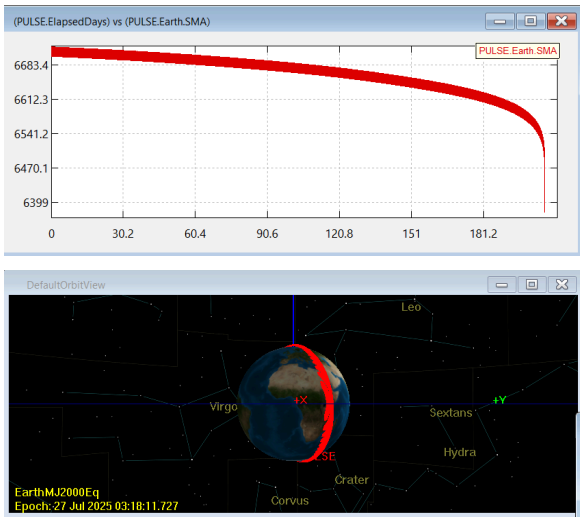

Figure 2.6. GMAT Results on PULSE

PULSE re-enters the atmosphere on 27th July 2025, 7 months after launch.

2.6. Mission Analysis

Mission analysis is simulated using above mentioned criteria. GMAT 2022 was used to calculate the following parameters for orbit height of 350 km.

- Mission lifetime
- Eclipse time around Earth
- Ground station contact time

Mission lifetime was estimated at 208 days or approx. 7 months with 93.75% of the duration in useful orbit for data collection and validation.

Earth eclipse data			
Total Eclipse incidents	Maximum duration (sec)	Average duration (sec)	Total eclipse time (days)
3318	2134.907	1918.743	73.685

Table 2.1. Earth Eclipse Data for PULSE Throughout Lifetime

Eclipse time is estimated at 35.42% of the mission lifetime. Hence, the power generation from the solar panels has to be at least 135.42% of the required power for one duty cycle. This would ensure that batteries are charged parallel to payload data acquisition. This would aid in estimation of duty cycle based on the power generated.

Ground Station Contact Time				
Sr. No.	Ground station.	Contact instances	Avg Contact time (sec)	Total contact time (days)
1	Berlin	854	336.65	3.32
2	Brandenburg	854	338.34	3.34
3	Backnang	714	299.106	2.47
4	Buenos Aires	644	335.71	2.50
5	Svalbard	2562	360.37	10.68
6	San Martin Base	1645	335.93	6.396

Table 2.2. Ground Station Contact Time for Mission Duration

As expected the ground stations at the poles have higher contact instances. Communication protocols need to be planned keeping these values in mind. The average contact duration is significant for metadata transfer using a duplex transfer protocol. Further analysis needs to be done on whether telecommand is possible during the transfer of high value image files. The conducted mission analysis shows that the PULSE satellite is a viable mission during the peak solar maximum period and is suitable enough to carry out the mission requirements.

3. POWER SYSTEM

The Electrical Power System (EPS) comprises 4 subsystems namely Power generation, Power storage, Power conversion and Power distribution. Altogether the EPS shall deliver a maximum of 12.42 Watts of power at the rate of 3.6V and 3.45A. Given below are the detailed description of each subsystem and its functions.

3.1 Power Generation - (Solar Array & MPPT)

Considering the power requirements,a total of 137 solar cells with 25% efficiency factor can fulfill the power demand. Each solar cell shall generate 0.56V and 55mA current. Figure 3.1 and 3.2 shows the 3P solar array arrangement for maximum and medium power generation sides which can generate 1.1W & 1.075W each side.

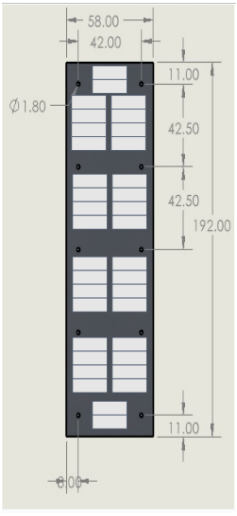

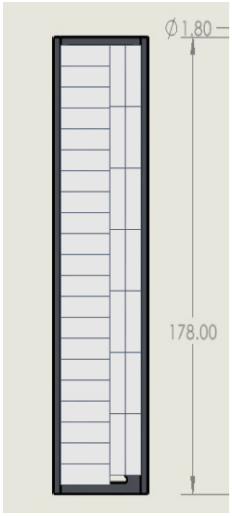

Figure 3.1 ***Figure 3.2***

Similarly, Figure 3.3 and 3.4 shows the 3P and 1P solar array arrangement for the minimum power generation sides which can generate 0.86W and 0.15W

Table 3.1 describes the orbital parameters and the power calculations of the solar cell arrays.

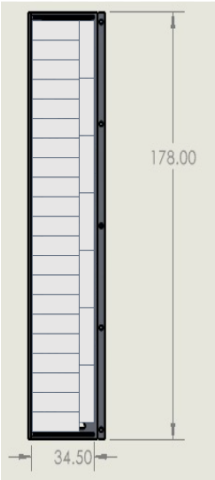

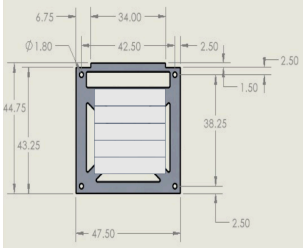

Figure 3.3 *Figure 3.4*

Parameter	Value
Orbit Height	350 Km
Inclination	97°
RAAN	351,6299°
Eclipse time	35.93 minutes
Day time	126.914 minutes
Minimum power without Albedo	0.13W
Maximum power without Albedo	0.94W

Table 3.1

In addition, the SPV1040 device is connected to the output terminal of the solar cells which is a low power, low voltage, monolithic step-up converter with an input voltage range from 0.3 V to 5.5 V, capable of maximizing the energy generated by solar cells (or fuel cells), where low input voltage handling capability is extremely important. It is also embedded with MPPT (Maximum Peak Power Tracker) which employs a voltage regulation loop, which fixes the charging battery voltage via a resistor divider.

3.2. Power Storage - (Battery & BMC)

Two Lithium-Ion cells of 3450mAh each are selected from Panasonic NCR18650GA model as the battery.

Table 3.2 and Figure 3.5 describe the specifications and the discharge characters of the battery.

Specifications		
Rated capacity(1)		3300mAh
Capacity(2)	Minimum	3350mAh
	Typical	3450mAh
Nominal voltage		3.6V
Charging	Method	CC-CV
	Voltage	4.20V
	Current	Std. 1475mA
	Time	Std. 270 min.
Weight (max.)		48.0g
Temperature	Charge	10 to +45° C
	Discharge	-20 to +60° C
	Storage	-20 to +50° C
Energy density(3)	Volumetric	693 Wh/l
	Gravimetric	224 Wh/kg

Table 3.2

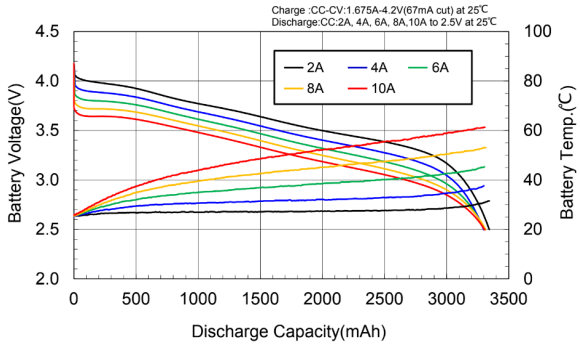

Figure 3.5

Both the cells are connected by the combination of two battery management circuits and isolation switches to charge and discharge the cells in an alternative sequence. This also provides the cold redundancy feature in an event of a single cell failure.

In addition to the battery, the BQ25638 device is a highly-integrated 5-A switch-mode battery charge management and system power path management device for single cell Li-Ion and Li-polymer batteries. Figure 3.6 illustrates the charging profile.

The power path management regulates the system slightly above battery voltage but does not drop below the programmable minimum system voltage. With this feature, the system maintains operation

even when the battery is completely depleted or removed. When the input current limit or input voltage limit is reached, the power path management automatically reduces the charge current. If the system load continues to increase, the power path discharges the battery until the system power requirement is met. This supplement mode prevents overloading the input source. The device also provides a 12-bit (ADC) analog-to-digital converter for monitoring charge current and input voltages. In addition, the ADCIN pin can be used to monitor an external signal up-to 1V. The cell switching is performed by the OBC (On Board Computer) by triggering the TPS22996N isolation switches.

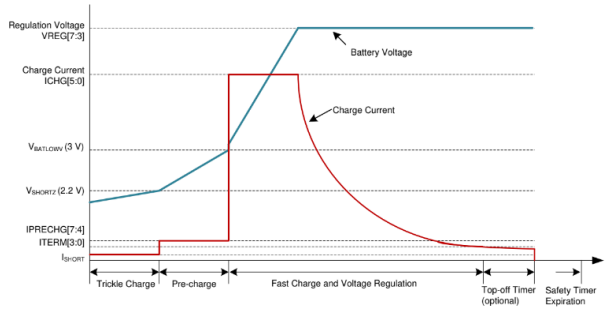

Figure 3.6

Finally, the TPS22996 represents a versatile load switch, boasting a 5.5-V capacity, dual-channel functionality, and low typical resistance at 14 milliohms in an 8-pin DRL package. Each channel handles up to 4 A of continuous current, controlled effortlessly by GPIO-compatible inputs.

3.3 Power Conversion

The power conversion subsystem includes two units of DC-DC converter and power monitor to regulate power supply for all the other systems of the satellite. The Texas Instrument's TLV61070A device is a synchronous boost converter with 0.5-V ultra-low input voltage. The DC-DC convertor provides a power supply solution by supplying 5.5V and 3.3V for various power demands in the satellite. A total of two 5.5V and one 3.3V DC-DC converter is used to fulfill the power requirements. The output voltage of the DC-DC convertor can be adjusted by the On Board Computer.

The second part of the power conversion subsystem consists of two units of Texas Instrument's INA3221 power monitor which is a three-channel, high-side current and bus voltage monitor with an I2C- and SMBUS-compatible interface. The INA3221 monitors both shunt voltage drops and bus supply voltages, in addition to having programmable conversion times and averaging modes for these signals. The INA3221 offers both critical and warning alerts to detect multiple programmable out-of-range conditions for each channel.

Figure 3.7 illustrates the functional block diagram of the power monitor.

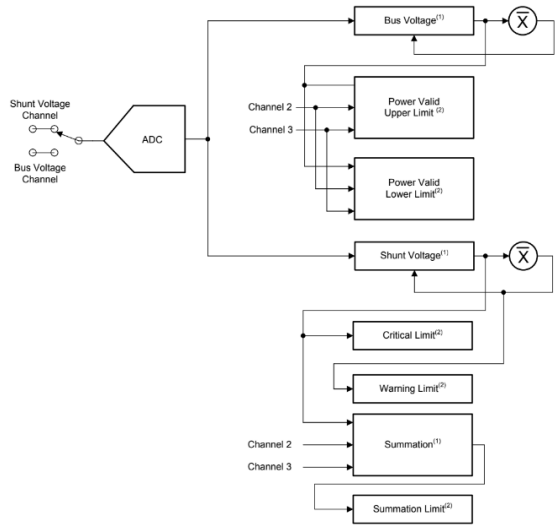

Figure 3.7

3.4 Power Distribution

The power distribution subsystem is the final stage of power supply to meet the power demands of various satellite systems. Eight individual TPS22996N isolation switches from texas instruments are controlled by the On Board Computer, controlling the power distribution to various satellite systems as per the modes and demands. Table 2.3 illustrates the power demand of the satellite system and Table 2.4 illustrates the activity state of various operational modes.

System / Sub-System	Operational Mode	Power Demand

ADCS	Standby	0.01W
TT&C	Data Link	4W
Payload	Full-Power (Science)	1.8W
EPS	Safe & Standby	~0.1W
OBC	All Modes	~0.5W

Table 3.3

System / Sub-System	Low Power Science	Full Power Science	Link	Stand By	Safe
ADCS	OFF	OFF	ON	ON	OFF
OBC	ON	ON	ON	ON	ON
TT&C	OFF	OFF	ON	OFF	OFF
Payload	ON	ON	OFF	OFF	OFF
Thermal	OFF	OFF	ON	ON	ON
EPS	ON	ON	ON	ON	ON

Table 3.4

The functional block diagram of all the EPS subsystems is illustrated in the figure 3.8 for power generation and power storage, While figure 3.9 illustrates power conditioning and distribution

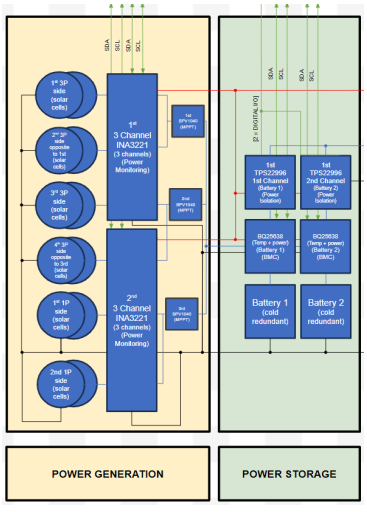

Figure 3.8

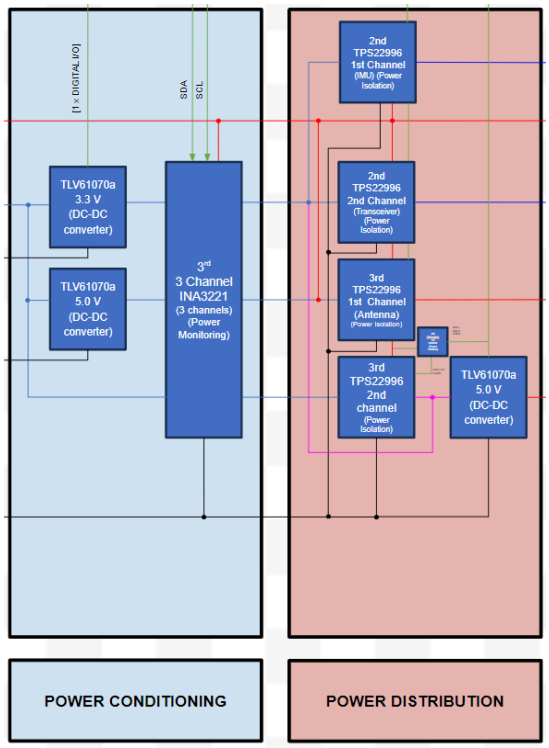

Figure 3.9

3.5 Fault Tolerance and Protection

The EPS system is embedded with several fault tolerance and protection features in order to prevent any single point failures in the satellite.

The fault tolerance and protection devices includes primarily the structure earthing to protect against electrical faults during assembly, integration, testing and transportation. Secondly the cold redundant secondary battery shall replace the primary battery in an event of high load and temperature faults. Additionally, it also increases mission lifetime twice. Thirdly, the redundant kill switches physically isolate the EPS with the rest of the systems and subsystems during assembly, integration, testing and transportation. Fourthly there is an additional regulated 5.5V supply which can automatically switch over to the secondary 5.5V converter in the event of the primary 5.5V DC-DC converter failure. Finally there is also an unregulated 3.6V supply which can automatically switch over as a substitute 3.3V converter in the event of the primary 3.3V DC-DC converter failure.

4. COMMUNICATION SYSTEM

The Telemetry, Tracking, and Command (TT&C) system for both the satellite and ground station is designed with specific parameters. The satellite system is designed to transmit with an output power of 16 dB at 50 ohms impedance, achieve an RF sensitivity of -109 dB at 38.4 Kbps, and support downlink and uplink speeds of 9.6 Kb/s and 4.8 Kb/s, respectively. It operates within a power consumption limit of less than 4W, weighs under 100 grams, and maintains functionality within a range of 600 km, utilizing a frequency of 435 MHz. Moreover, it incorporates a release mechanism for deployable antennas and employs the SPI communication protocol with the On-Board Computer (OBC).

The ground station system, on the other hand, features an output power of 22 dB, employs cross Yagi antennas, includes a transceiver unit and a ground station computer, and shares similar specifications in terms of data rates, power consumption, range, and frequency. Both systems rely on the Technische Universität Berlin (TU-Berlin) Ground Station Architecture.

4.2 Transceiver Module

The transceiver module chosen to be integrated in the PULSE satellite is an off-the-shelf RC-SPIRIT2-433 module (shown in figure 4.1), leveraging the STMicroelectronics S2-LP transceiver. It is a high-performance, ultra-low-power RF transceiver, it targets RF wireless applications operating in the sub-1GHz band. This module, designed for compactness with dimensions of 11.5mm x 13.5mm, offers 4 programmable I/O pins and features a metal shield for SMD mounting. Its operational frequency band is approximately centered around 435 MHz, and it can be programmed via SPI interface by an external microcontroller.

Figure 4.1 - RC-SPIRIT2-433 module

Furthermore, the S2-LP Device incorporates hardware support for Gaussian Frequency Shift Keying (GFSK) modulation scheme, along with error correction and detection mechanisms. Data can be processed using convolutional coding (rate 1/2) or interleaving Forward Error Correction (FEC), although FEC coding is mutually exclusive with Manchester and Three-out-of-six coding. Additionally, the S2-LP features a highly adaptable and programmable packet handler, facilitating packet construction based on user-defined configuration settings. Supported packet types include BASIC format, STACK format with auto acknowledgment and auto retransmission, 802.15.4g packet format, and UART over-the-air packet format. Meanwhile, the antennas (shown in figure 4.2) will be deployable, exhibiting flexibility and possess a 50 ohms impedance. They can be constructed from either polycarbonate and copper or ITO (Indium Tin Oxide) and silver conductive ink.

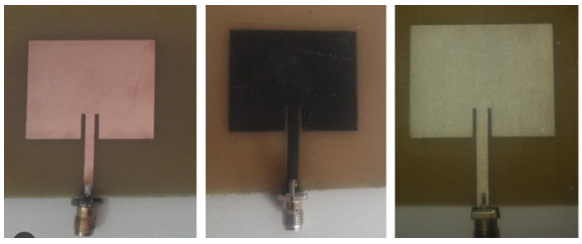

Figure 4.2 - Antenna concept for PULSE

4.1 Link Budget

For the PULSE satellite, the link budget parameters are listed in table 4.1, the link budget calculations are listed in table 4.2 and the link budget results are listed in table 4.3

Parameter	Uplink Value	Downlink Value
Range	600 Km	600 Km
Frequency	435 MHz	435 MHz
Tx power	22 dBW	2 dBW
Elevation	10°	10°
Antenna Efficiency	65%	65%
Data rate	10000 Kbit/s	10000 Kbit/s

(Tx / Rx) gain	(0 / 0) dB	(0 / 22) dB
Required Eb / Eo	14	14
Bit Error Rate	10-6	10-6
Implementation loss	2 dB	2 dB
Free Space Loss	153.93 dB	153.93 dB
Total loss	155.93 dB	155.93 dB

Table 4.1 - Link Budget Parameters

Item	Value
Received Power	-111.0310818 dB
Receiver Power at Receiver	-78.74108176 dB
Sensitivity of Transmitter at 38kbps	-110 dB
Margin with Sensitivity	31.25891824 dB
Carrier Phase Noise (Worst Case Scenario)	-125 dB
SNR	13.96891824 dB
SNR Minimum (Noise Figure)	8 dB
Total Margin of Satellite	5.968918244 dB

Table 4.2 - Link Budget Calculations

Item	Uplink Value	Downlink value
Radiated power	100W	1.6W
Bit Rate	10000 Kbit/s	10000 Kbit/s
System Temperature	500K	1839.77K
Peak Receive Antenna Gain	22 dB	2 dB
Carrier to Noise Density Ratio	17.59 dB	16.05dB
Link Margin	6.4161 dB	6.9604 dB

Table 4.3 - Link Budget Results

4.3 TT&C Functional Block Diagrams

Figure 4.1 illustrates the functional block diagram of the RC-SPIRIT2-433 transceiver module of the PULSE satellite. Communication between the S2-LP and MCU occurs via a standard 4-wire SPI interface and utilizes 4 GPIOs, including a SHUTDOWN pin. The MCU is capable of various operations, including programming the S2-LP in different operating modes through command transmission, reading data from the RX FIFO and writing data into the TX FIFO, configuring the S2-LP through its registers, retrieving information from the S2-LP, handling interrupt requests and signals from GPIO pins such as OBC reset, applying external signals to GPIO pins, and transitioning the S2-LP between shutdown and active states.

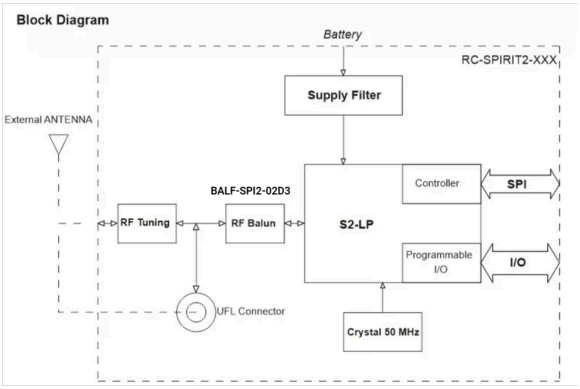

Figure 4.1 - Transceiver Block Diagram

Similarly, figure 4.2 illustrates the TT&C functional block diagram of the TU-Berlin ground segment.

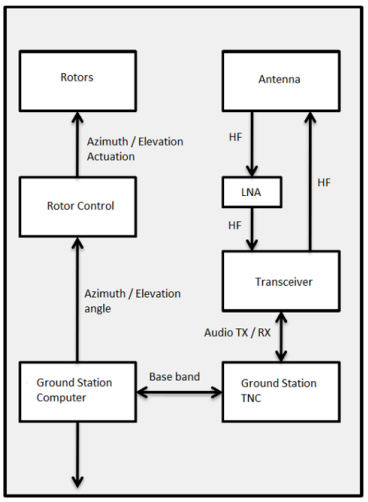

Figure 4.2 - Ground Segment Block Diagram

5. ATTITUDE DETERMINATION & CONTROL

For ADCS systems in a PocketQube the major constraints in the systems are weight and size restrictions introduced by the PocketQube standard [15]. The standard restricts the weight of a 3P PocketQube to 750 grams and dimensions to 50x50x178 mm. ADCS is comparatively a bulky system and requires heavy computing power and electrical power.

To get around this, embedded air coils technology is used for de-tumbling and minimum pointing requirements to suffice the telecommunication requirements, since the payload cannot determine the particle incident angle or direction anyway, the payload is not optimized to find the source of the particle flux and hence doesn't require attitude data to calibrate. Embedded air coils use the capability to be printed on the back of solar panels, hence being compact and producing low magnetic torque enough to dampen the system. Technische Universität Berlin has prior experience building satellites with embedded aircoils for BeeSat and NanoFF. TU Berlin has also developed a software to wrap the coils in a PCB to get the required torque.

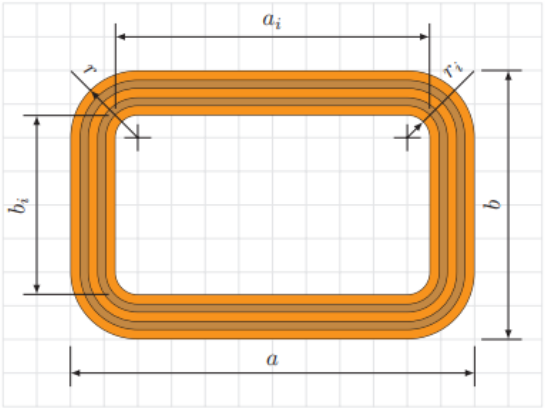

Figure 5.1 Embedded AirCoil Illustration

$$\tau = \mu \times B, \qquad (1)$$

$$\mu = Vc\mathcal{M} + I \sum m\ i{=}1\ niAi\ , \qquad (2)$$

$$P = U \text{ x } I = U^2 / R\ . \qquad (3)$$

Equations (1), (2) & (3) discuss the power (P) required to produce torque (τ) for dipole vector (μ) that interacts with Earth magnetic field (B). *Vc* is core volume, $\mathcal{M}$ is core magnetization, *I* is current through the coil, *m* is number of differently shaped windings, *ni* is number of turns for each type and A_i is the enclosed area [15]. Plugging in the values for the PULSE subsystem reveals a current requirement between 28 - 40 mA/m^2 with 150 mW power, which is not high and manageable with available power.

6. ON-BOARD DATA-HANDLING

PULSE's core operations are centralized through the robust On-board Computer (OBC) NXP i.MX6, powered by a Quad Core ARM Cortex-A9 processor. To enhance reliability and mitigate risks, a cold redundancy strategy was implemented, equipping the spacecraft with a secondary OBC. This backup unit remains inactive but fully functional, ready to take over in the unlikely event of a primary OBC failure.. This OBC is essential for carrying out critical operations such processing telemetry packets received from ground stations, analyzing sensor data from the ADS and EPS, and issuing orders to manage the Payload's various modes. A significant feature of the mission is precise timekeeping, achieved through an external RTC. The OBC is equipped with a 1MB L2 cache, 64-bit DDR3, and a 16GB eMMC memory, ensuring reliable storage for all housekeeping data and payload information.

The OBC makes use of the SPI and I^{2}C protocols, which are combined with necessary buses to allow for easy subsystem integration. A task manager, alongside watchdog and timers, forms the backbone of the OBC's software architecture, providing tight oversight over all modes and services, improving error detection capabilities and allowing for system reset via telecommand or watchdog in the event that a process becomes unresponsive.

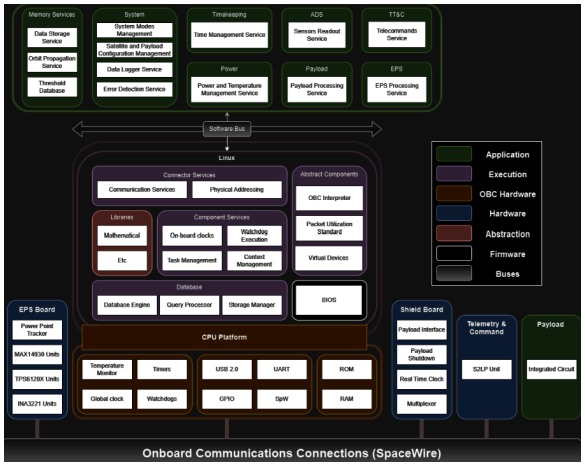

Figure 6.1 - OBDH Functional Diagram

6.1. On-board Software architecture (OBSW)

The software architecture begins with the hardware layer encompasses all critical units such as TT&C, Payload, EPS (where it is important to note the EPS Processing Service includes the necessary capabilities to multiplex all I^2C signals), the external PCB shield board, and the OBC itself, which includes timers, clocks, watchdogs, I/O interfaces, and memory hardware. Ascending from this base, the firmware and abstraction layers facilitate seamless interaction between the hardware and higher software tiers. In the execution layer, task management and context management systems are in place. This layer is also equipped with watchdogs and timers, enhancing system reliability. The on-board clocks ensure precise timekeeping, crucial for mission operations. An OBC interpreter bridges the gap between hardware signals and software instructions. The execution layer also houses the Packet Utilisation Standard (PUS) for consistent data handling, along with a database engine, a query processor, and a storage manager.

At the top, the application layer features a suite of services crucial for mission success. This includes a data storage service for efficient information handling, an orbit propagation service, that in conjunction with the RTC information, provides the proper trajectory information. Furthermore, the threshold database service for operational parameters. System mode management ensures optimal operational states, while a data logger and error detection services maintain system integrity. Time management service, EPS processing, power and temperature management services, and sensor readout are vital for system coordination and environmental monitoring. Telecommand service facilitates ground communication, and payload processing handles scientific data. The software bus that connects all of these parts allows for reliable and efficient data transfer across the various layers, guaranteeing an efficient and well-coordinated operation.

7. STRUCTURE SYSTEM

The structure adheres to ESA guidelines and ECSS Standards, embodying precision in design and adherence to constraints. With dimensions of 178 * 50 * 50 mm^3 and a mass of 450g, the satellite features a structured frame, including a sliding backplate (178 * 50 mm^2), three side panels, and two top and bottom panels, all with a 0.75 mm thickness. Panels are interconnected by 1.25 mm brackets along vertical sides, enhancing structural integrity.

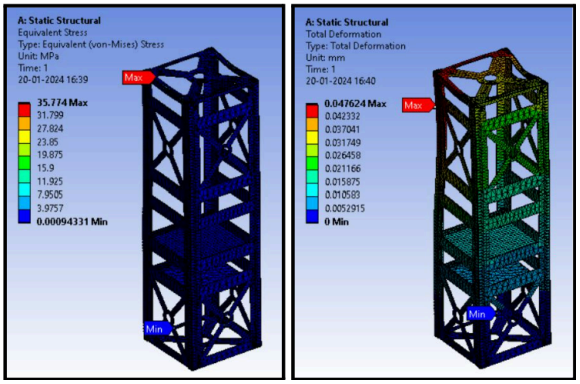

Figure 7.1 - Preliminary structure analysis

Aluminum 6061 is chosen for its availability, strength, and cost-effectiveness. The x-cross section design, coupled with horizontal supports, ensures a lightweight yet robust structure. The center of mass, critical for stability, is meticulously kept within 1 cm in the stowed position. Metallic materials in contact with the deployer and standoffs undergo hard anodization.

Each 3P PocketQube adheres to a 750g mass limit as per standards. Safety is a priority, with kill switches exclusively on the Z-axis. Placement options include the lateral side within 20 mm from Z-faces, touching deployment rails, or aligned with the sliding backplate in Z-face, contacting the PocketQube

below or the pusher plate. Kill switches do not obstruct ejection.

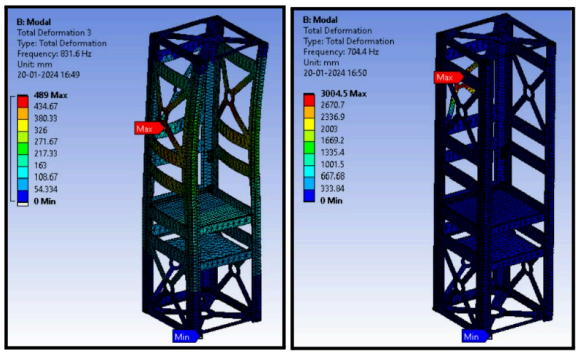

Figure 7.2 - Preliminary Modal Analysis & Equivalent Stress Distribution

Structural simulations were performed to analyze stress distribution and deformation under various loads and conditions, ensuring the satellites robustness during launch and in orbit. Modal simulations were performed to assess natural frequencies and vibration responses, for understanding the PocketQube's dynamic behavior. For Structural Simulations, extruded legs at the bottom represent the fixed support that will make contact with the P-Pod's lower boundary. Vertical as well as Side Tension Test was simulated which showed that the structure can withstand mechanical loads, ensuring material integrity for using Aluminum 6061.

For modal analysis, a spring-loaded deployment mechanism is used in the P-POD.This spring-loaded design allows for a very small amount of vertical movement during launch, while the side rails keep the satellite rigidly fixed in two directions. Because of this for the boundary conditions, the side of the PocketSat was constrained in all directions other than the vertical direction as it allowed the structure to warp slightly during takeoff, and will simulate the rigid sides of the P-POD.The results achieved through this simulations were satisfied as the first mode values were 704 Hz which is much greater than major forcing amplitudes in launch vehicles that occur below 100Hz.

7.1. Antenna Deployment System

The satellite uses a foldable antenna system that is safely mounted during launch with the help of a nylon wire inside the deployer. Interference with neighboring satellites is then avoided. The antenna unfolds when the heating coil properly melts the nylon wire upon release. Once the nylon wire melts, a micro switch is built to cut off the current to the heating coils, protecting the batteries and guaranteeing a safe deployment procedure.

8. CONCLUSION

The proposed satellite PULSE presents a new area of opportunity to better investigate space weather effects during solar events in LEO. PocketQubes while promising cost-wise for large scale constellations, volume and weight constraints prove a challenge in duty cycle limitations because the power generated is low. However, with a creative approach with operational mode strategy and in selecting relevant data to downlink, this could potentially be overcome. This mission has the potential to open new possibilities for PocketQubes and educational applications if successfully demonstrated.

ACKNOWLEDGEMENTS

We are grateful to Advacam for sponsoring the MiniPix Sprinter payload and to our mentors Katerina and David. We would also like to thank all our advisors at TU Berlin, especially Cem Avsar and Sebastian Trowitzsch for all their support. Finally, we would like to thank our classmates and core PULSE team members who contributed to this body at work.

REFERENCE

1. Miteva et al. (2023).Space Weather Effects on Satellites. Astronomy. 2023; 2(3):165-179, https://doi.org/10.3390/astronomy2030012
2. Ray et al. (2022). The impact of space weather on very low Earth orbit (VLEO) satellites. Advanced Maui Optical and Space Surveillance Technologies (AMOS), https://www.researchgate.net/publication/364677851_The_impact_of_space_weather_on_very_low_Earth_orbit_VLEO_satellites
3. Reitz, G. (2008). Characteristic of the radiation field in low earth orbit and in deep space,

4. Trichtchenko et al. (2014). Highly Elliptical Orbits for Arctic observations: Assessment of ionizing radiation. Advances in Space Research. 54. 10.1016/j.asr.2014.09.012.
5. Johnson et al. (2014). AE9/AP9/SPM: New Models for Radiation Belt and Space Plasma Specification, https://www.vdl.afrl.af.mil/programs/ae9ap9/files/publications/20140603_SPIE_Johnston_AE9AP9_Overview.pdf
6. Virtual Distributed Laboratory (2023). IRENE-AE9/AP9/SPM Radiation Environment Model. Known Issues and Limitations (Version 1.57.004). https://www.vdl.afrl.af.mil/programs/ae9ap9/issues-and-limits.php, accessed on 18 Jan 2024.
7. Werner, D. (2019). Are small satellites the solution for space weather monitoring? 2019 https://spacenews.com/are-small-satellites-the-solution-for-space-weather-monitoring/
8. Bouwmeester et al. (2020). Utility and constraints of PocketQubes. CEAS Space J 12, 573–586 (2020). https://doi.org/10.1007/s12567-020-00300-0
9. Furnell et al. (2019). First results from the LUCID-Timepix spacecraft payload onboard the TechDemoSat-1 satellite in Low Earth Orbit. Advances in Space Research, Volume 63, Issue 5, 2019, pages 1523-1540, ISSN 0273-1177, https://doi.org/10.1016/j.asr.2018.10.045.
10. Murphy et al. (2021). A compact instrument for gamma-ray burst detection on a CubeSat platform I: Design drivers and expected performance. Exp Astron (Dordr). 2021;52(1-2):59-84. doi: 10.1007/s10686-021-09779-9.
11. Kovar et al. (2022). Demonstration of the Capability of 1U CubeSat for Measurement of the Energy Spectrum on LEO. Electronics. 2022; 11(20):3390. https://doi.org/10.3390/electronics11203390
12. Granja et al. (2022). Directional-Sensitive X-ray/Gamma-ray Imager on Board the VZLUSAT-2 CubeSat for Wide Field-of-View Observation of GRBs in Low Earth Orbit. Universe. 2022; 8(4):241. https://doi.org/10.3390/universe8040241
13. Reid, Tyler. (2017). Orbital Diversity for Global Navigation Satellite Systems.
14. Badhwar, G. D. (1997). The Radiation Environment in Low-Earth Orbit. *Radiation Research*, *148*(5), S3–S10. https://doi.org/10.2307/3579710
15. PocketQube Standard by Alba Orbital & TU Delft published on june 7, 2018